RESEARCH ARTICLE

Editorial Process: Submission:10/03/2025 Acceptance:05/01/2026 Published:05/19/2026

In Vitro Anticancer Activity of Green-Synthesized Zinc Oxide Nanoparticles from Root Extract of *Sida schimperiana* against MDA-MB-231 Breast Cancer Cell Lines

Asmelash Hagos[1], Zenebe Hagos[1], Berihu Tekluu[1], Tesfay Welderfael[1], Naveen Kumar A.D[2], Kamalakararao Konuku[3], Krishna Chaithanya K[1]*

Abstract

Objective: This work addressed the fact that nano phytoformulations have emerged as promising, biocompatible alternatives to conventional cancer drugs, helping to overcome drug resistance in cancer and offering sustainable, biocompatible, and effective drug delivery. This study aimed to synthesize zinc oxide nanoparticles (SS-ZnO NPs) using an eco-friendly green synthesis method from Sida schimperiana aqueous root extract (SS-AQ), and to evaluate their selective cytotoxicity against MDA-MB-231 breast cancer cells. **Methods:** The SS-ZnO NPs were characterized using spectroscopic (FTIR, XRD, DLS), microscopic (SEM, TEM), and chemical (EDX) analytical techniques. The selective cytotoxicity of SS-ZnO NPs against breast cancer cell lines (MDA-MB-231) and normal cell lines (L929) was evaluated using the MTT assay. **Results:** XRD analysis confirmed that SS-ZnO NPs possess a crystalline, hexagonal wurtzite structure with an average size of 55.4 nm. DLS analysis indicated that the SS-ZnO NPs are monodispersed with a negative surface charge of –28.9 mV, suggesting high colloidal stability. SEM and TEM-EDX analyses revealed that the SS-ZnO NPs exhibit a pseudo-spherical, rough morphology with an average particle size of 22.65 nm. Strong absorption peaks at 1.01 keV and 0.52 keV were observed, corresponding to the characteristic signals of Zn and oxygen, respectively. The MTT assay demonstrated that SS-ZnO NPs exhibited significant, dose-dependent selective cytotoxicity against MDA-MB-231 breast cancer cell lines, with inhibition ranging from 10.14% to 62.44% at concentrations of 6.25–100 µg/mL, and an IC_{50} value of 45.28 µg/mL ($p \leq 0.01$). In comparison, SS-AQ exhibited 8.81% to 58.11% inhibition at the same concentration range, with an IC_{50} of 50.16 µg/mL ($p \leq 0.01$). **Conclusion:** The findings of the current study highlight that bio-inspired SS-ZnO NPs possess enhanced anticancer properties and can be considered a promising anticancer agent with potent, specific cytotoxic efficacy against MDA-MB-231 breast cancer cells, offering a potential alternative nanotherapeutic approach with reduced toxicity.

Keywords: Anticancer- Breast Cancer- Green Synthesis- ZnO Nanoparticles- Sida schimperiana

Asian Pac J Cancer Prev, **27 (5)**, 1845-1854

Introduction

Nano-oncology has emerged as a one of the most cutting-edge interdisciplinary fields of the twenty-first century, combining clinical oncology and advanced materials science, with applications in timely identification, efficient therapy, real-time monitoring, and targeted drug delivery to specific cancer sites [1]. Researchers around the world have invested a lot of capital, time, and expertise in the production and manipulation of nonmaterials at the nanoscale (1-100 nm) [2]. These nanomaterials have received prodigious attention due to their exceptional physicochemical, electrical, optical, magnetic, catalytic, and biological properties by tailoring features such as large surface area and quantum confinement [3]. For a long time, the scientific community has developed various physical and chemical methods to generate nanomaterials with high purity, scalability, controlled particle size, and a wide range of applications [4]. However, contempt of their use, these traditional methods frequently present significant challenges, such as high energy consumption, environmental pollution, high costs, and the use of toxic reducing agents [5]. To address these challenges, researchers have developed sustainable, environmentally friendly, and cost-effective approaches based on green chemistry principles, plant-mediated nanoparticle synthesis stands out as a promising alternative to traditional methods [6].

*[1]Department of Chemistry, College of Natural and Computational Sciences, Aksum University, Axum, Ethiopia. [2]Department of Biochemistry, University College of Science and Technology, Adikavi Nannaya University, Rajamahendravaram, Andhra Pradesh, India. [3]School of Medicine, Texila American University, Lusaka, Zambia, Central Africa. *For Correspondence: Krishnachaithanyawc07@gmail.com*

The phytosynthesis method successfully uses secondary metabolites such as polyphenols, flavonoids, terpenoids and tannins as reducing, stabilizing, and capping agents [7]. These secondary metabolites, with their diverse functional groups, not only act as active medical agents, but also helps in advancing cancer therapeutics including enhanced biocompatibility, improved bioavailability, controlled drug release, increased stability, multifunctionality, and precise dosing [8]. Among various metal oxide nanoparticles, zinc oxide nanoparticles (ZnONPs), are used for developing novel nano-drugs for breast cancer treatment [9], also, ZnONPs are believed to effectively combat breast cancer progression due to their unique physicochemical properties, that include high surface area, biocompatibility, and ease of functionalization, which enable targeted drug delivery, increased bioavailability, and potent anticancer activity in a short period of time [10]. Green-synthesized ZnONPs interact with cancer cells acidic microenvironment, releasing zinc ions as well as phyto-compounds that enable the mitochondria-dependent intrinsic apoptotic pathway [11].

Sida schimperiana is a medicinal plant from the Malvaceae family that distributed widely in Ethiopia, Kenya, Uganda, Tanzania, and Eritrea, and widely used as traditional medicine to treat many kinds of ailments, including wounds, respiratory infections, fever, intestinal disorders, malaria, joint pain, coughs, colds, asthma, stomach aches, and skin diseases [12]. Phytochemical analysis of Sida species such as Sida acuta and Sida rhombifolia revealed the presence of secondary metabolites such as alkaloids, flavonoids, saponins, and phenolic compounds [13]. These compounds demonstrated for their significant biological properties such as antioxidant, anticancer, anti-inflammatory, antibacterial, and antifungal activities, highlighting the genus' therapeutic potential [13-15].

According to current World Health Organization (WHO) reports, breast cancer will remain the leading cause of cancer-related deaths in women worldwide in 2023. Approximately 2.3 million new cases of breast cancer were diagnosed in 2022, about 685,000 deaths worldwide [16]. Globally, one in eight women is diagnosed with breast cancer at some point in her life, and one in any eleven dies from the disease [17]. Despite the clinical effectiveness of chemotherapy regimens as a primary treatment strategy for breast cancer, there are several major drawbacks, including insufficient drug absorption, systemic toxicity, a lack of specificity [18], and the rapid emergence of multidrug resistance in breast cancer tissues. These challenges point out the critical need for novel therapeutic approaches that improve treatment efficacy, minimize side effects, and improve patient outcomes [19]. Metal oxide nanoparticles, particularly ZnONPs synthesized using novel nano-phytoformulations have showed promising anticancer activity by activating intrinsic apoptotic pathway by inhibiting proliferation, and decreasing adverse effects.

Therefore, to the best of our knowledge, the present study was first attempt to green synthesize SS-ZnO NPs using an aqueous root extract of *Sida schimperiana* (*S.schimperiana*) as a reducing and capping agent. These obtained SS-ZnO NPs were characterized using spectroscopic, microscopic techniques furthermore; these SS-ZnO NPs were evaluated for their potential in vitro selective cytotoxicity against MDA-MB-231 human breast cancer cell lines.

Materials and Methods

Chemicals and reagents

Zinc acetate dihydrate ($Zn(CH_3COO)_2 \cdot 2H_2O$) (99.9%) (Sigma-Aldrich; USA), Dimethyl sulfoxide (DMSO), (Sigma-Aldrich; USA), Phosphate-buffered saline (PBS), Dulbecco's modified Eagle's medium (DMEM) (Thermo Fisher Scientific; USA), fetal bovine serum (FBS),(Thermo Fisher Scientific; USA), Trypsin-EDTA solution (Thermo Fisher Scientific; USA)Penicillin/Streptomycin (Thermo Fisher Scientific; USA) 3-(4,5-dimethylthiazol-2-yl)-2,5-diphenyltetrazolium bromide (MTT), (Thermo Fisher Scientific; USA). All solvents and chemicals used in the experiments were of analytical grade and were purchased from local suppliers.

Collection, Authentication and Preparation of Plant extract

Fresh *Sida schimperiana* (S. schimperiana) roots were collected in February 2021 from Axum City, Tigray region, Ethiopia, authenticated and assigned the voucher specimen number AH-001 by a botanist Mr. Melaku Wendaferash at the National Herbarium of Ethiopia, Addis Ababa University. The roots were washed with running tap water, followed by distilled water, and then shade-dried at room temperature for two weeks. According to the modified methodology of Chaithanya et al. [20] a Soxhlet extractor was used to extract approximately 100 g of powdered root material (1:5 w/v) over three cycles for 8 hours using 500 mL of distilled water. After extraction, the plant extract was filtered using Whatman filter paper No. 1. The filtrates were concentrated at 50–60°C using a rotary evaporator under reduced pressure [21]. The percentage yield of each extract was calculated using the following formula:

$$\text{Percentage yield} = \frac{\text{Extract weight of the plant (g)}}{\text{Dry weight of the plant (g)}} \times 100 \quad (1)$$

Qualitative Phytochemical Screening

Preliminary phytochemical analysis was performed to detect various phytochemical constituents, including alkaloids, phenolic compounds, flavonoids, tannins, saponins, steroids, glycosides, terpenoids, and anthraquinones, in the aqueous root extract of S. schimperiana using standard methods described by Harborne and Williams [22].

Green Synthesis of SS- ZnONPs

A green synthesis of SS-ZnO NPs was carried out using the aqueous root extract of *S.schimperiana*, by following a modified protocol of Wafaeyet al. [23]. In brief, 10 mL of sterile aqueous root extract of S. schimperiana was added drop wise with continuous stirring to 90 mL of a 1 mol/L solution of zinc acetate dihydrate ($Zn(CH_3COO)_2 \cdot 2H_2O$),

at a temperature of 60–80°C. The mixture was stirred magnetically at 300 rpm for 15 minutes. The resulting solution was centrifuged at 3,500 rpm for 10 minutes to remove unreacted plant extract. The green-synthesized nanoparticles were then collected by centrifugation at 12,000 rpm for 20 minutes. The synthesized SS-ZnO NPs, were allowed to dry in a watch glass at 50–60°C followed by further purification through continuous washing with sterile distilled water to obtain pure SS-ZnO NPs in pellet form. The colour change of the reaction mixtures was the initial indication of SS-ZnO NP formation. Dimethyl sulfoxide (2% DMSO) was used to dissolve the S. schimperiana root aqueous extract (SS-AQ) and SS-ZnO NPs. Stock solutions were prepared in DMEM culture medium at a concentration of 1 mg/mL. The final DMSO concentration never exceeded 0.1% after filtration of the prepared samples using 0.2 µm porous membrane filters.

Characterization of SS- ZnONPs

According to Gholami Shabani et al. [24] and Joudeh and Linke [25], the obtained SS-ZnO NPs were validated using spectroscopic and microscopic techniques. A noticeable colour change was observed, indicating the formation of nanoparticles. UV-Vis spectroscopy (Shimadzu) was performed in the range of 200–800 nm to confirm the surface plasmon resonance (SPR) peaks of SS-ZnO NPs. FT-IR (IRTracer-100, Shimadzu) analysis was conducted in the range of 400–4000 cm^{-1} to identify functional groups present in the aqueous root extract of S. schimperiana and the surface chemistry of SS-ZnO NPs, which act as reducing and capping agents. X-ray diffraction (XRD-6100, Shimadzu) analysis was performed in the range of 5° to 80° to determine the crystalline structure. Dynamic Light Scattering (DLS) and zeta potential analyzers (Zetasizer Nano ZS) were used to measure the size distribution and zeta potential of the nanoparticles. Scanning Electron Microscopy (SEM) coupled with Energy Dispersive X-ray Spectroscopy (EDS) (Shimadzu) was used to analyze the surface morphology and elemental composition of SS-ZnO NPs. Transmission Electron Microscopy (TEM) (Zeiss EM10 C, 100 kV) was used to analyze the internal morphology and size of the nanoparticles.

Cell Cultures and Maintenance

MDA-MB-231 (breast carcinoma) and normal mouse fibroblast cell line (L929) were purchased from the American Type Culture Collection (ATCC). These stock cell lines were cultured in 24-well plates with RPMI-1640 supplemented with 10% heat-inactivated fetal bovine serum (FBS), streptomycin (100 µg/mL), penicillin (100 Units/mL), and 2 mM L-glutamine, maintained at 37°C in a 90% humidified 5% CO_2 atmosphere incubator until they reached 80% confluence.

In vitro Cytotoxicity Activity

The selective in vitro cytotoxic effect of the UV-sterilized aqueous crude root extract of S. schimperiana (SS-AQ) and its green-synthesized SS-ZnO NPs against MDA-MB-231 (breast carcinoma) and normal mouse fibroblast L929 cell lines were determined by the MTT colorimetric reduction assay (3-(4,5-dimethylthiazol-2-yl)-2,5-diphenyl tetrazolium bromide dye) according to the modified methods of Mfengwana and Bertrand [26]. These cell lines were seeded at a density of 1×10^4 cells/well in a flat-bottom 96-well plate in complete DMEM and incubated for 24 hours at 37°C in a humidified atmosphere of 95% air with 5% CO_2. After 24 hours, the cells were subsequently treated with five different concentrations of SS-AQ and SS-ZnO NPs (6.25, 12.5, 25, 50, and 100 µg/mL). Cisplatin (2.5, 5, 10, 20, and 40 µg/mL) was used as a positive control. These treatments were added to each well in triplicate, except for the basal control wells, where only nutrient medium (DMEM) was added. The plates were incubated for 24 hours in a 5% CO_2 incubator at 37°C. Following the incubation period, 20 µl of MTT (5 mg/ml) reagent was added to each well and incubated for 4 hours in the dark in a 5% CO_2 incubator at 37°C. After incubation, the MTT reagent was aspirated, and 100 µl of 10% Sodium Dodecyl Sulfate (SDS) was added, leading to the formation of purple-coloured formazan products. The absorbance was measured spectrophotometrically using a micro-ELISA plate reader at 570 nm. Cytotoxicity was determined using the following formula, and IC_{50} values were calculated:

Cytotoxicity (%) = (OD of control-OD of test)/ (OD of control) ×100 (2)

To determine the selective cytotoxicity of SS-AQ, SS-AuNPs, and SS-ZnO NPs against the L929 and MDA-MB-231 cell lines, the selective index (SI) was calculated using the given equation.

Selective Index (SI)= (IC_{50} of normal cell lines)/(IC 50 of cancer cell lines) ×100 (3)

Statistical analysis

Statistical differences between the Mean ± SD values of the anticancer activity (% cell viability) between the control (without plant extract) and experimental group was assessed by using unpaired Student's t-test. Statistical analysis were performed using Microsoft Excel 2007 and Graph Pad Prism version 9.0, with statistical significance indicated as *$p < 0.05$, **$p < 0.01$, and ***$p < 0.001$ versus control.

Results

Percentage of yield

As shown in Table 1, the percentage yield of the aqueous root extract of S. schimperiana was 10.5%, extract appeared a dark brown colour with a slightly viscous nature. These results are consistent with Donkor et al. [27], who reported that the aqueous leaf extract of Sida acuta had highest percentage yield of 9.3%.

Qualitative phytochemical analysis

The preliminary phytochemical analysis of the aqueous root extract of S. schimperiana revealed the moderate presence of alkaloids, phenolic compounds, tannins, and flavonoids, and the minimal presence of

Table 1. Colour, Consistency and Percentage of Yield (w/w %) of Aqueous Root Extract of *S.schimperiana*

Extract	Colour	Consistency	Percentage of yield
Aqueous extract of root of S.schimperiana	Dark brown	Slightly viscous	10.50%

Table 2. Qualitative Phytochemical Screening of Aqueous Root Extract of *S. schimperiana*

Chemical constituents	Test	Result
Alkaloid	Mayer's test	++
Phenolic compound	Ferric chloride test	++
Tannins	Ferric chloride test	++
Flavonoids	Alkaline reagent test	++
Steroid	Liebermann–Buchard's test	+
Saponins	Foam test	+

+, Minor presence; ++, Moderate presence

steroids and saponins (Table 4), which are responsible for the bioreduction of Zn^{2+} ions to Zn^0 during the synthesis of SS-ZnO NPs. Additionally, these compounds also act as stabilizing and capping agents, preventing agglomeration of SS-ZnO NPs. Our results align with the previous phytochemistry Sida species reported by Membe et al. [13], who indentified simalr secondary metabolites alkaloids, flavonoids, tannins, phenolic compounds, sterols, and triterpenes in hydroethanolic extracts of Sida acuta (whole plant) and *Sida rhombifolia* (aerial parts) (Table 2).

Characterization of SS-ZnO NPs

Visual Colour Change Observation

As depicted in Figure 1, the formation of ZnONPs from the aqueous root extract of S. schimperiana was initially confirmed by the observed colour changes from colourless to light brown. This colour change revealed the bio-reduction of Zn^{2+}ions to Zn^0, leading to the synthesis of biogenic SS-ZnO nanoparticles. The characteristic colour change is due to specific optical properties of SS-ZnO nanoparticles, including quantum confinement, localized surface plasmon resonance (LSPR) [28].

Our results align with previous reports of Chai et al. [29], observed similar colour changes from colourless to light brown, confirming the formation of zinc oxide nanoparticles (ZnO NPs) from Hibiscus rosa-sinensis flower extract through bioreduction of Zn^{2+} ions to Zn^0.

UV-Vis Spectroscopy of SS-ZnO NPs

The optical properties of SS-ZnO NPs in solutions were measured using UV-Vis spectroscopy in the wavelength range of 200–800 nm. As shown in Figure 2, the UV-Vis spectra of SS-ZnO NPs showed a wide absorption range between 300 to 400 nm, with a distinct peak at 330 nm, which corresponds to the oscillation of free conduction band electrons in zinc oxide nanoparticles. The results align with findings of Mongy and Shalaby [30], who reported that ZnO NPs prepared from Rhuscoriaria fruit aqueous extract exhibited maximum absorbance at approximately 359 nm.

FT-IR Analysis

The FT-IR spectrum provides information about the functional groups present in the aqueous root extract of *S.schimperiana* responsible for the bio-reduction, stabilization, and synthesis of SS-ZnO NPs (Table 3).

Figure 3, show the FTIR spectrum of SS-ZnO NPs, indicating the presence of characteristic stretching frequency peaks at 3653, 3481, 2494, 2181, 2032, 991, and 445 cm^{-1}, corresponding to their respective functional groups: O-H (hydroxyl group), N-H (amines or amides), S-H (thiols), C≡C (alkynes) / C≡N (nitriles), C≡C (conjugated alkynes), C=O (carbonyl in conjugation) / C=C (aromatic or alkenes), =C-H (alkenes), and Zn-O (zinc-oxygen bond). These functional groups on the surface of SS-ZnO NPs may be responsible for the bio-reduction and stabilization of Zn^{2+} ions to Zn^0 and help prevent the agglomeration of SS-ZnO NPs. Similar results were reported by Mongy and Shalaby [30] for synthesis of R. coriaria fruit extract-mediated ZnO NPs. Our findings also supported by previous reports of Ifeanyichukwu et al. [31].

XRD Analysis

The XRD patterns of SS-ZnO NPs are shown in Figure 4, showed characteristic peaks at 2θ values of

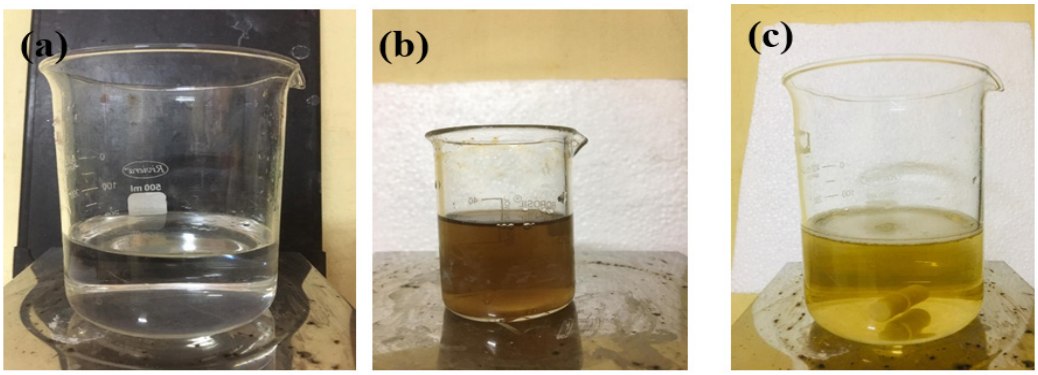

Figure 1. The Colour Changes during Green Synthesis of SS-ZnO NPs with Aqueous Root Extract of *S. schimperiana* (a) Zinc(II) acetate dehydrate solution; (b) Aqueous root extract of *S. schimperiana* ; (c) SS-ZnO NPs

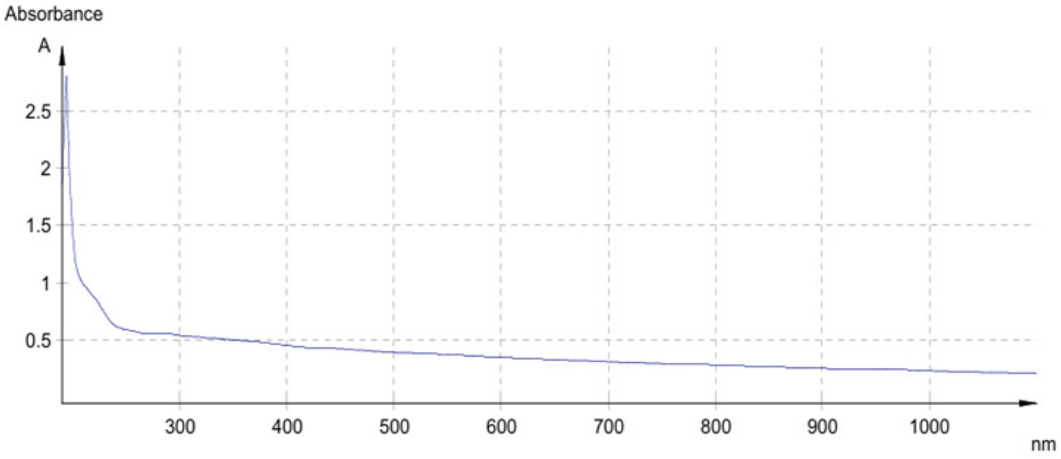

Figure 2. UV-Vis Analysis of SS-ZnO NPs Prepared from Aqueous Root Extract of *S.schimperiana*

31.7º, 34.4 º, 36.2º, 47.5 º, 56.6 º, 62.8º, 67.9º and 72.5º corresponding to the lattice planes (100), (002), (101), (102), (110), (103), (112), and (201) respectively. These diffraction peaks align with hexagonal wurtzite crystalline structure of zinc oxide (ZnO), as confirmed by the JCPDS card No. 36-1451. The calculated average crystallite size, based on the Debye-Scherer equation, yielded an average value of 55.4 nm, indicating a relatively small crystallite size for SS-ZnO NPs.

Furthermore, the XRD pattern of SS-ZnO NPs agrees with Faisal et al.,[32], who reported that zinc oxide nanoparticles synthesized from aqueous fruit extracts of Myristica fragrans also exhibited peaks corresponding to the (100), (002), (101), (102), (110), (103), and (112) planes. This comparison further confirms the hexagonal wurtzite structure of ZnO nanoparticles.

Dynamic Light Scattering (DLS) analysis

The particle size distribution of SS-ZnO NPs was determined using a dynamic light scattering (DLS) by measuring light interference based on the Brownian motion of NPs dispersed in a liquid medium. This method measures the size distribution based on the polydispersity index of NPs, which ranges from 0 to 1.

The dynamic light scattering (DLS) analysis of SS-ZnO NPs as shown in Figures 5, revealed a distinct size distribution. SS-ZnO NPs had an average size of 396.2 nm within the same range, with a higher polydispersity index (PDI) of 0.865, suggesting greater size variability. Our findings similar with Faisal et al. [32] reported that ZnO NPs from the aqueous extract of Myristica fragrans was (45.3 nm) with a PDI of 0.5, indicating a more uniform distribution.

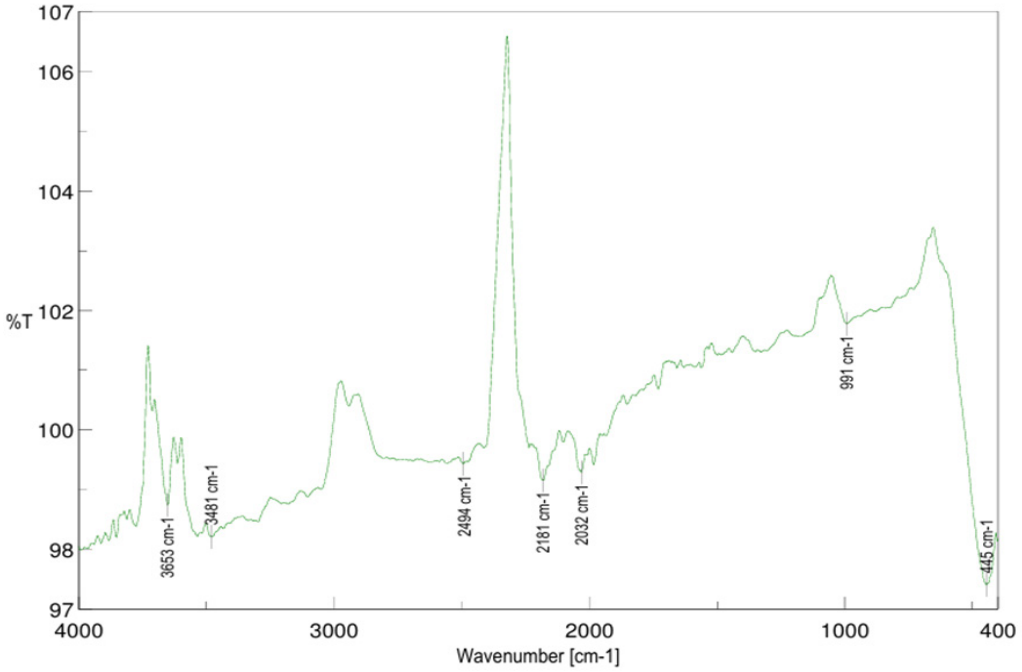

Figure 3. FT-IR Spectrum of Green Synthesized SS-ZnO NPs from Aqueous Root Extract of *S.schimperiana* by potassium bromide (KBr) pellet method and, scanned wave number range of 400- 4000 cm^{-1}

Table 3. FT-IR Chemical Finger Printing and Vibrations of SS-ZnO NPs from Aqueous Root Extract of *S.schimperiana*

Wave number (cm^{-1})	Functional Group / Bond	Vibration Mode
3653	O-H (free hydroxyl group)	Stretching (sharp, strong)
3481	N-H (amines)	Stretching (broad for O-H)
2494	S-H (thiols)	Stretching (medium to weak)
2181	C≡C (alkynes) / C≡N (nitriles)	Stretching (sharp)
2032	C≡C (conjugated alkynes)	Stretching (medium, sharp)
991	=C-H (alkenes)	Out-of-plane bending (medium)
445	Zn-O(Zinc-Oxygen bond)	Stretching (lattice vibrations)

Zeta potential analysis

As shown in Supplementary Figure 1, SS-ZnO NPs showed a zeta potential of –28.9 mV, indicating high colloidal stability. The negative zeta potential helps prevent agglomeration, by electrostatic repulsion. However, with a value close to the stability threshold range of -20 mV to +20 mV, the colloidal stability may decrease over time. Our findings are consistent with Kaliyaperumal et al. [33], who reported a zeta potential of -27.1 mV for ZnO NPs from Phyllanthus emblia extract, equally indicating stable dispersions.

EDAX Analysis

As shown in Supplementary Figure 2, the EDX spectrum of SS-ZnO NPs, showed characteristic peak for Zn at 1.01 keV, while the oxygen peak at 0.52 keV, confirm the presence of Zn-O bonding and the formation of ZnO nanoparticles.

Our results were similar with previous reports of Jaishi et al. [34],who reported that ZnO NPs synthesized using the aqueous bark extract of A. nepalensis D. Don displayed a strong EDX peak for zinc at approximately 1 keV, verifying the ZnO composition.

SEM Analysis

As shown in Supplementary Figure 3, the SEM images of SS-ZnO NPs, revealed a pseudo-spherical morphology with a rough and rocky surface appearance. The nanoparticles exhibited irregularities and flake-like structures, indicative of partial aggregation during green synthesis. The rough and flaky morphology may be attributed to the ZnO nuclei fusing under the influence of bioactive compounds from the extract. Ahmad and Kalra [35] reported similar results for ZnO nanoparticles prepared with using the leaf extract of Euphorbia hirta, which also showed a pseudo-spherical shape with a few aggregates.

TEM Analysis

As shown in Supplementary Figure 4, TEM analysis of SS-ZnO NPs showed a pseudo-spherical morphology, consistent with negligible aggregation, with size ranging from 13 nm–38.6 nm and an average size of 22.65 nm. These findings demonstrate the ability of S. schimperiana root extract to produce nanoparticles with precise morphologies and sizes, demonstrating its potential for green nanotechnology applications.

Jamdagni et al. [36] reported that ZnO NPs synthesized using Nyctanthes arbor-tristis flower extract had a size range of 12–32 nm.

Table 4. Comparative Selective Cytotoxic Effect and IC_{50} Values of SS-AQ, and SS-ZnO NPs on MDA–MB-231cell Lines and Normal L929 Fibroblast Cells

Extracts /Standard	Concentration (µg/mL)	% Cytotoxicity		IC50 (µg/mL)		Selective Index (SI)
		MDA-MB 231	L929	MDA-MB 231	L929	
SS-AQ	6.25	8.11 ±044	5.22±0.11	50.16	>100	
	12.5	19.19±0.11	8.22±0.01			1.99
	25	26.11±0.63	12.10±0.96			
	50	44.09±0.96	14.11±0.85			
	100	58.11±0.93	15.96±0.05			
SS-ZnO NPs	6.25	10.14±0.10	5.55±0.16			
	12.5	21.34±0.38	10.54±0.14	45.28		2.2
	25	31.22±0.18	13.81±0.53		>100	
	50	48.34±0.40	15.22±0.12			
	100	62.44±0.26	18.31±0.03			
Cisplatin	2.5	18.15±38	ND	8.34	ND	ND
	5	39.74±29	ND			
	10	56.69±0.43	ND			
	20	77.09±0.19	ND			
	40	91.74±0.76	ND			

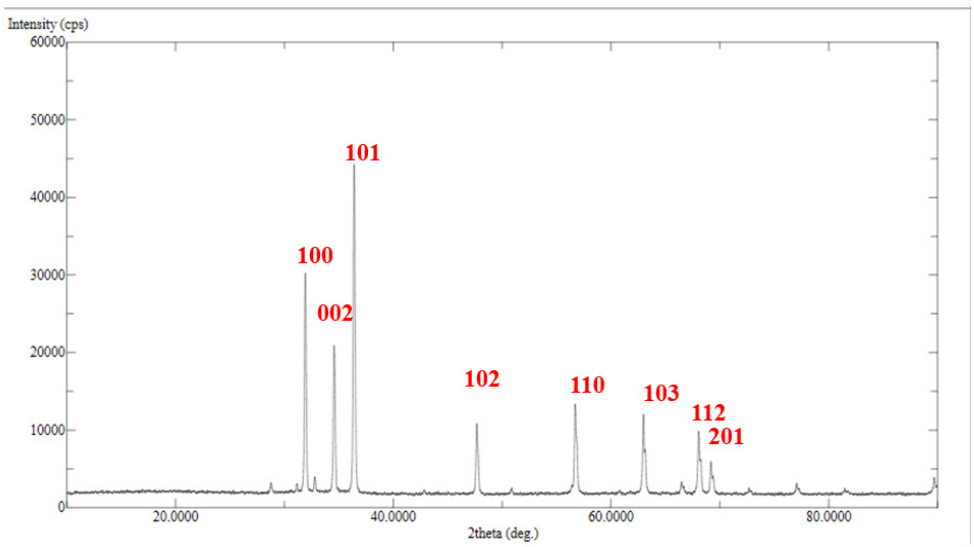

Figure 4. XRD Spectra of SS-ZnO NPs from Aqueous Root Extract of *S. schimperiana* Recorded in the 2θ Range of 10°–80° Using Cu Kα Radiation (λ = 1.5406 Å).

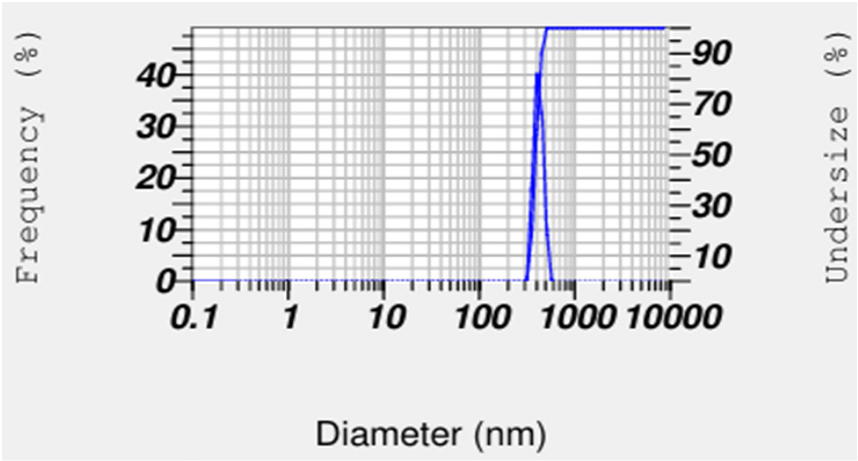

Figure 5. Particle Size Distribution of SS-ZnO NPs from Aqueous Root Extract of *S. schimperiana* by DLS Analysis was Performed at 25°C Using a 633 nm

Cytotoxicity Analysis of SS-ZnO NPs on MDA MB-231 Cell Lines

Preliminary MTT assay results showed that SS-ZnO NPs and the aqueous root extract of *Sida schimperiana* (SS-AQ) exhibited dose-dependent selective cytotoxicity against MDA-MB-231 breast cancer cells and normal L929 fibroblast cells over 24 hours. As shown in Supplementary Figure 5, SS-ZnO NPs showed significantly higher selective anticancer activity against MDA-MB-231 cells ($p < 0.01$) compared to SS-AQ. The highest inhibition of 62.44% and 58.11% were observed respectively at a dosage of 100 µg/mL with significance of ($P < 0.01$) with IC_{50} values of 45.28µg/mL and 50.16µg/mL against MDA-MB-231.

Cisplatin used as a standard showed cytotoxicity between 18.15% to 91.74% at doses of 2.5–40 µg/mL with an IC_{50} value of8.34 µg/mL. Both SS-ZnO NPs and SS-AQ showed minimal cytotoxicity of in the range of 5.22% –15.96% and 5.55%-18.31%respectivelyat concentrations of 6.25 – 100µg/mL with $IC_{50}$of >100indicating their biocompatibility with non-cancerous cells. The selective cytotoxic activity of SS-ZnO NPs and SS-AQ against MDA-MB-231 cells followed this order:

SS-ZnO NPs> SS-AQ

The selective index (SI) values of SS-ZnO NPs, and SS-AQ against MDA–MB-231 cells, compared to L929 cells, were 2.22, and 1.99, respectively (Table 4). SS-ZnO NPs showed a cytotoxic concentration (CC50) >100 µg/mL in L929 cells and an IC_{50} of 45.28 µg/mL in MDA–MB-231 cells, resulting in an SI of 2.2 This indicates that SS-ZnO NPs exhibited preferential cytotoxicity toward MDA–MB-231 cells, sparing normal cells. The high SI of SS-ZnO NPs confirms their anticancer potential against aggressive triple-negative breast cancer, likely due to their optimal size, shape, charge, and secondary metabolites like phenolic compounds, tannins, and flavonoids from *Sida schimperiana*. The factors such as enhanced cellular uptake, oxidative stress, ROS generation, mitochondrial damage, contribute apoptosis in MDA–MB-231 cells [37].

Effect of SS-ZnO NPs on Cells Morphology

Morphological analysis of MDA-MB-231 cells treated with SS-ZnONPs revealed significant apoptosis-related changes in a dose-dependent manner. Cells were exposed to ½ IC_{50} (20 µg/mL), IC_{50} (40 µg/mL), and 2× IC_{50} (80 µg/mL) for 24 hours. As shown in Supplementary Figure 6, cellular shrinkage, membrane blebbing, detachment, and apoptotic body formation were prominent at IC_{50} and 2× IC_{50}, confirming apoptosis and SS-ZnONPs' cytotoxicity.

Discussion

Medicinal plants have extended played important role in traditional medicinal system for treatment of various cancers. Earlier research studies demonstrated that the isolated bioactive compounds Vinblastine, Capsaicin, Resveratrol and Lycopene from various medicinal plants showed potential anticancer activity by targeting and modulating different enzymatic, molecular mechanism and signal transduction pathways [38]. Hence in the present study roots of *S.schimperiana* were selected based on traditional use in Ethiopia medicinal system and earlier phytochemical studies demonstrated that presence of various secondary metabolites are capable of exhibiting various pharmacological activities, such as modulating cancer-related pathways in a line with significant ethno botanical evidence from Gedeo Zone and Amhara region, Ethiopia [39].

In this study first time we successfully green-synthesized high stable, pseudo-spherical shape, with average size of 22.65 nm from the aqueous crude root extract of *S.schimperiana* (SS-AQ). The results evident that SS-ZnONPs' demonstrated significant dose-depended selective cytotoxicity against MDA-MB-231 cell lines with promising IC_{50} of 45.28 µg/mL while aqueous crude root extract of *S.schimperiana* (SS-AQ) also showed comparable strong selective cytotoxicity against MDA-MB-231 cell lines with IC_{50} of 50.16 µg/mL. Hence introducing green, synthesized ZnO NPs from green sources like *S.schimperiana* roots rich in secondary metabolites will have great impact on nano medicine discovery, increased bioavailability, cost effective and less adverse effect compared to currently available chemotherapeutic agents.

ZnO NPs posses exceptional physicochemical properties such as high surface area, abundant surface defects, mechanical stability and enhanced electron mobility that enable integrated in bio medical system, for target drug delivery, carries medicine and facilitate the controlled release of nanomedicine at precise sites [40]. To support our results, different latest publication of green synthesis of ZnO NPs evident that ZnO NPs can exhibit their biological applications as antibacterial, antifungal, antidiabetic, anti-oxidant, anti-inflammatory and anticancer agents. Sishu and Selvaraj, green synthesized ZnO nanoparticle from root aqueous extract Cichorium intybus L produced average size of 26.66 nm with quasi-spherical particles that showed, significant DPPH radical scavenging (60.63 µg/mL), anti-diabetic by inhibiting α-amylase (41.74 µg/mL), showing strong anticancer activity on anticancer A549 lung cancer cell lines (26.56 µg/mL) and biocompatible properties by low hemolysis supporting their biomedical potential [41]. Akhras et al. [42], similarly reported that ZnO NPs prepared from aqueous extract of Artemisia absinthium L. exhibited strong antibacterial and antifungal activities against tested Staphylococcus aureus, Escherichia coli, and Candida albicans.

The present study aligns with existing reports by Mongy and Shalaby [30] who reported that zinc oxide nanoparticles (ZnO NPs) produced from Rhus coriaria fruit extract, showed dose-dependent anticancer activity with IC_{50} values ranging from 35.04–44.86 µg/mL against MCF-7 cells and 55.54–63.71 µg/mL for MDA-MB-231 cells.In line with these findings, Ahamed et al. [37], reported that ZnO NPs synthesized from Phoenix dactylifera fruit extract showed enhanced anticancer activity against MCF-7 cells compared to pure ZnO NPs, highlighting the potential of plant-derived nanoparticles in cancer therapies, especially for triple-negative breast cancer. This study employed an eco-friendly, phyto-mediated approach to synthesize SS-ZnO NPs using the aqueous root extract of *Sida schimperiana* (SS-AQ) as a reducing and capping agent. The successful formation of SS-ZnO NPs was confirmed by distinct colour changes in the reaction medium. Phytochemical and FTIR analyses revealed that bioactive compounds such as phenolics, tannins, and flavonoids played a crucial role in reducing Zn^{2+} to Zn^{0}, and stabilizing the nanoparticles via surface functionalization. Characterization studies demonstrated that SS-ZnO NPs were crystalline, predominantly pseudo-spherical, with average sizes of 22.65 nm.

In conclusion, the findings of current study confirmed that SS-ZnO NPsexhibited superior selective anticancer activity against MDA-MB-231 cells compared to SS-AQ extract without

effecting normal cell lines highlighting the potential of green-synthesized SS-ZnO NPs as promising biogenic nanotherapeutic agents and drug delivery tool against aggressive breast cancer therapies.

Author Contribution Statement

Asmelash Hagos, Zenebe Hagos and Kamalakararao K conducted the experimental workand acquisition of all the data in Department of Biology and Chemistry. Berihu Tekluu, Tesfay Welderfaeland Naveen Kumar A.Dinvolved in collection of review of literature, draftingmanuscript and editing. Krishna Chaithanya K performedstatistical analysis and organized manuscriptaccording to the submission guidelines of Journal.

Acknowledgements

The authors would like to thank the Department of Biology and Chemistry, Post Graduate Directorate, Research Directorate of Aksum University and Ethiopian Ministry of Education for funding this research.

Funding statement

This student research work was partially funded by Post Graduate Research Directorate, Aksum University,

Ethiopia.

Scientific Approval

It is a part of an approved student thesis

Ethical Declaration

There is no involvement of human participants or animals hence did not require ethical approval.

Data availability statement

All data supporting the finding of this study are included within the article.

Conflict of interest

The authors declare that they have no conflict of interest.

References

1. Jiang j, cui x, huang y, yan d, wang b, yang z, et al. Advances and prospects in integrated nano-oncology. Nano biomed eng. 2024;16(2):152-87. Https://doi.Org/10.26599/nbe.2024.9290060
2. Elzein B. Nano revolution: "Tiny tech, big impact: How nanotechnology is driving sdgs progress". Heliyon. 2024;10(10):e31393. https://doi.org/10.1016/j.heliyon.2024.e31393.
3. Vancha H, Ansari MM, Devesh T, Awadh Bihari Y, Neelesh S, Sweta B, et al. Cutting-edge advances in tailoring size, shape, and functionality of nanoparticles and nanostructures: A review. J Taiwan Inst Chem Eng. 2023;149:105010. https://doi.org/10.1016/j.jtice.2023.105010.
4. Saxena S, Chauhan SB. Nanomaterial synthesis using tyre and plastic. 2024. p. 325-50.
5. Chen L, Zhang Y, Chen Z, Dong Y, Jiang Y, Hua J, et al. Biomaterials technology and policies in the building sector: A review. Environ Chem Lett. 2024;22(2):715-50. https://doi.org/10.1007/s10311-023-01689-w.
6. Rathod S, Preetam S, Pandey C, Bera SP. Exploring synthesis and applications of green nanoparticles and the role of nanotechnology in wastewater treatment. Biotechnol Rep (Amst). 2024;41:e00830. https://doi.org/10.1016/j.btre.2024.e00830.
7. Nagar R, Mathur P, Chaturvedi P, Sharma C, Bhatnagar P. Secondary metabolites in green synthesis of nanoparticles. In: Microbial approaches for sustainable green technologies. Boca Raton: CRC Press; 2024. p. 287-303.
8. James J, Verma M, Sharma N. Nanotechnology-driven improvisation of red algae-derived carrageenan for industrial and bio-medical applications. World J Microbiol Biotechnol. 2023;40(1):4. https://doi.org/10.1007/s11274-023-03787-x.
9. Ullah R, Siraj M, Zarshan F, Abbasi BA, Yaseen T, Waris A, et al. A comprehensive overview of fabrication of biogenic multifunctional metal/metal oxide nanoparticles and applications. Reviews in Inorganic Chemistry. 2025;45(2):411-36.
10. Alhaddad R, Abualsoud BM, Al-Deeb I, Nsairat H. Green synthesized zingiber officinale-zno nanoparticles: Anticancer efficacy against 3d breast cancer model. Future Sci OA. 2024;10(1):2419806. https://doi.org/10.1080/20565623.2024.2419806.
11. Naser SS, Ghosh B, Simnani FZ, Singh D, Choudhury A, Nandi A, et al. Emerging trends in the application of green synthesized biocompatible zno nanoparticles for translational paradigm in cancer therapy. J Nanotheranostics. 2023;4(3):248-79.
12. Yeabyo s, teka zm, gopalakrishnan vk, kamalakararao k, muthulingam m, chaithanya kk. Immuno protective potential of sida schimperiana chloroform root extract against e. Coli 018: K1 induced peritonitis in albino wistar rats. Res j pharm technol. 2021;14(4):2262-9. . https://doi.org/10.52711/0974-360X.2021.00400
13. Membe Femoe U, Kadji Fassi JB, Boukeng Jatsa H, Tchoffo YL, Amvame Nna DC, Kamdoum BC, et al. In vitro assessment of the cercaricidal activity of sida acuta burm. F. And sida rhombifolia linn. (malvaceae) hydroethanolic extracts, cytotoxicity, and phytochemical studies. Evid Based Complement Alternat Med. 2022;2022(1):7281144. https://doi.org/10.1155/2022/7281144.
14. Sengul U, Reneta G, Kouadio Ibrahime S, Aslı Ugurlu B, Yasemin Celik A, Dimitrina Z-D, et al. New perspectives into the chemical characterization of sida acuta burm. F. Extracts with respect to its anti-cancer, antioxidant and enzyme inhibitory effects. Process Biochem. 2021;105:91-101. https://doi.org/10.1016/j.procbio.2021.03.028.
15. Arciniegas A, Pérez-Castorena A-L, Nieto A, Kita Y, Romo A. Anti-hyperglycemic, antioxidant, and anti-inflammatory activities of extracts and metabolites from sida acuta and sida rhombifolia. Química Nova. 2016. https://doi.org/10.21577/0100-4042.20160182.
16. Wilkinson L, Gathani T. Understanding breast cancer as a global health concern. Br J Radiol. 2022;95(1130):20211033. https://doi.org/10.1259/bjr.20211033.
17. Henke A, Wacker J, N'Diaye A, Kantelhardt EJ. Malignant Diseases of Women Worldwide. InGlobal Women's Health: Gynecology and Obstetrics Under Diverse Global Conditions 2024 Dec 10 pp. 203-214. Berlin, Heidelberg: Springer Berlin Heidelberg.
18. Balisa Mosisa E, Malay KD, Sanjoy D. Recent advances in paclitaxel drug delivery: Challenges, innovations, and future directions. Journal of Angiotherapy. 2024;8(8). https://doi.org/10.25163/angiotherapy.889867.
19. Chen T, Xiao Z, Liu X, Wang T, Wang Y, Ye F, et al. Natural products for combating multidrug resistance in cancer. Pharmacol Res. 2024;202:107099. https://doi.org/10.1016/j.phrs.2024.107099.
20. Chaithanya KK, Gopalakrishnan VK, Zenebe H, Kamalakararao K, Patricia Ponce N, Dogulas PJ, et al. Isolation and structural characterization of bioactive anti-inflammatory compound mesuaferrin-a from m. Ferrea. Anal Chem Lett. 2019;9(1):74--85. https://doi.org/10.1080/22297928.2019.1573702.
21. Ashenafi E, Abula T, Abay SM, Arayaselassie M, Taye S, Muluye RA. Analgesic and anti-inflammatory effects of 80% methanol extract and solvent fractions of the leaves of vernonia auriculifera hiern. (asteraceae). J Exp Pharmacol. 2023;15:29-40. https://doi.org/10.2147/jep.S398487.
22. Harborne JB, Williams CA. Advances in flavonoid research since 1992. Phytochemistry. 2000;55(6):481-504. https://doi.org/10.1016/s0031-9422(00)00235-1.
23. Wafaey AA, El-Hawary SS, Abdelhameed MF, El Raey MA, Abdelrahman SS, Ali AM, et al. Green synthesis of zinc oxide nanoparticles using ethanolic extract of gliricidia sepium (jacq.) kunth. Ex. Walp., stem: Characterizations and their gastroprotective effect on ethanol-induced gastritis in rats. Bioorg Chem. 2024;145:107225. https://doi.org/10.1016/j.bioorg.2024.107225.
24. Gholami-Shabani M, Sotoodehnejadnematalahi F, Shams-Ghahfarokhi M, Eslamifar A, Razzaghi-Abyaneh M. Physicochemical properties, anticancer and antimicrobial activities of metallic nanoparticles green synthesized by aspergillus kambarensis. IET Nanobiotechnol. 2022;16(1):1-

13. https://doi.org/10.1049/nbt2.12070.
25. Joudeh N, Linke D. Nanoparticle classification, physicochemical properties, characterization, and applications: A comprehensive review for biologists. J Nanobiotechnology. 2022;20(1):262. https://doi.org/10.1186/s12951-022-01477-8.
26. Mfengwana PH, Sone BT. Green synthesis and characterization of ruthenium oxide nanoparticles using gunnera perpensa for potential anticancer activity against mcf7 cancer cells. Sci Rep. 2023;13(1):22638. https://doi.org/10.1038/s41598-023-50005-7.
27. Donkor AM, Ahenkorah B, Wallah TA, Yakubu A. Evaluation of extracts from sida acuta, phyllanthus amarus, parkia biglobosa and their herbal ointment for therapeutic and biological activities. Heliyon. 2023;9(9):e19316. https://doi.org/10.1016/j.heliyon.2023.e19316.
28. Basit M, Akram MA, Saleem M, Javed S, Koh JH. ZnO Nanoparticles as a Catalyst for Water Purification. InZinc Oxide Nanoparticles-Fundamentals and Applications 2024 Dec 10. IntechOpen. https://doi.org/10.5772/intechopen.1007849.
29. Chai HY, Lam SM, Sin JC. Green synthesis of ZnO nanoparticles using Hibiscus rosa-sinensis leaves extracts and evaluation of their photocatalytic activities. InAIP Conference Proceedings 2019 Sep 18 (Vol. 2157, No. 1, p. 020042). AIP Publishing LLC.
30. Mongy Y, Shalaby T. Green synthesis of zinc oxide nanoparticles using rhus coriaria extract and their anticancer activity against triple-negative breast cancer cells. Sci Rep. 2024;14(1):13470. https://doi.org/10.1038/s41598-024-63258-7.
31. Ifeanyichukwu UL, Fayemi OE, Ateba CN. Green synthesis of zinc oxide nanoparticles from pomegranate (punica granatum) extracts and characterization of their antibacterial activity. Molecules. 2020;25(19). https://doi.org/10.3390/molecules25194521.
32. Faisal S, Jan H, Shah SA, Shah S, Khan A, Akbar MT, et al. Green synthesis of zinc oxide (zno) nanoparticles using aqueous fruit extracts of myristica fragrans: Their characterizations and biological and environmental applications. ACS Omega. 2021;6(14):9709-22. https://doi.org/10.1021/acsomega.1c00310.
33. Kaliyaperumal V, Alharbi R, Rajendhran H, Gopal D, Alotibi F. Beta-cyclodextrin–phyllanthus emblica emulsion for zinc oxide nanoparticles: Characteristics and photocatalysis. Green Processing and Synthesis. 2024;13. https://doi.org/10.1515/gps-2024-0056.
34. Jaishi DR, Ojha I, Bhattarai G, Baraili R, Pathak I, Ojha DR, et al. Plant-mediated synthesis of zinc oxide (zno) nanoparticles using alnus nepalensis d. Don for biological applications. Heliyon. 2024;10(20):e39255. https://doi.org/10.1016/j.heliyon.2024.e39255.
35. Ahmad W, Kalra D. Green synthesis, characterization and anti microbial activities of zno nanoparticles using euphorbia hirta leaf extract. J King Saud Univ Sci. 2020;32. https://doi.org/10.1016/j.jksus.2020.03.014.
36. Jamdagni P, Khatri P, Rana JS. Green synthesis of zinc oxide nanoparticles using flower extract of nyctanthes arbor-tristis and their antifungal activity. J King Saud Univ Sci. 2016;30. https://doi.org/10.1016/j.jksus.2016.10.002.
37. Ahamed M, Akhtar MJ, Khan MAM, Alhadlaq HA. Enhanced anticancer performance of eco-friendly-prepared mo-zno/rgo nanocomposites: Role of oxidative stress and apoptosis. ACS Omega. 2022;7(8):7103-15. https://doi.org/10.1021/acsomega.1c06789.
38. Hashim GM, Shahgolzari M, Hefferon K, Yavari A, Venkataraman S. Plant-derived anti-cancer therapeutics and biopharmaceuticals. Bioengineering (Basel). 2024;12(1). https://doi.org/10.3390/bioengineering12010007.
39. Tewelde F. Ethnobotanical use and diversity of medicinal plants in zana and laelay koraro woredas, ethiopia. Sustainability Science and Resources. 2025;8:38-79. https://doi.org/10.55168/ssr2809-6029.2025.8003.
40. Kadhim R, Jabir M, Sulaiman G, Nayef U, Mohammed H, Abomughaid M. The advancing of zinc oxide and gold nanoparticles as a promising therapeutic approach for future biomedical applications. Plasmonics. 2025;20:10367-88. https://doi.org/10.1007/s11468-025-03134-w.
41. Nayan Kumar S, Chinnadurai Immanuel S. Bio-fabrication of cichorium intybus l. Root aqueous extract mediated zno nanoparticle (cirae-zno np) for its promising therapeutic applications. Green Chem Lett Rev. 2025;18(1):2489461. https://doi.org/10.1080/17518253.2025.2489461.
42. Akhras N, Çelekli A, Bozkurt H. Enhanced antimicrobial activity of green-synthesized artemisia-zno nanoparticles: A comparative study with pure zno nanoparticles and plant extract. Foods. 2025;14(14). https://doi.org/10.3390/foods14142449.